JOURNAL OF GEOPHYSICAL RESEARCH, VOL. 106, NO. D22, PAGES 28,699-28,710, NOVEMBER 27, 2001

Characteristics of cloud-nucleating aerosols in the Indian Ocean region

Cynthia H. Twohy,[1] James G. Hudson,[2] Seong-Soo Yum,[2] James R. Anderson,[3] Susan K. Durlak,[4] and Darrel Baumgardner[5]

Abstract. During the Indian Ocean Experiment (INDOEX), cloud droplets were collected and evaporated using a counterflow virtual impactor (CVI). The nonvolatile residual particles were then analyzed by various instruments. Physical and chemical properties of the cloud droplets and their residual nuclei were compared with properties of the below-cloud aerosol to evaluate which aerosol particles act as cloud nuclei in different environments, and their effects on cloud microphysics. Four cases, ranging from clean Southern Hemispheric clouds to heavily polluted clouds near India, were analyzed. For the cleaner clouds, droplet concentrations were a much higher fraction of the available particle concentrations than for polluted clouds, but entrainment apparently acted to reduce droplet number concentrations in both regimes. For clean clouds the median critical supersaturation and size of the ambient particles and droplet residual particles were similar. In polluted clouds there were stronger differences between ambient and droplet residual distributions, and particles with lower critical supersaturations were favored as nuclei. Simple model calculations were used to show that polluted clouds are expected to achieve lower water supersaturations than clean clouds; thus only particles with relatively low critical supersaturations are likely to affect clouds in polluted regions. Soluble fractions for the ambient aerosol inferred from the size and cloud condensation nuclei measurements were in general agreement with another study in the region. Droplet residual particles did not necessarily have higher soluble fractions than the ambient aerosol, but did tend to have higher total amounts of soluble material per particle, particularly in the polluted cases.

1. Introduction

Of critical importance in predicting climate change are the indirect effects of aerosol particles on clouds. Anthropogenic particles can act as cloud condensation nuclei (CCN) and subsequently affect climate through changes in cloud albedo [*Twomey*, 1977a] and lifetime [*Albrecht*, 1989]. Our limited knowledge of these processes handicaps our ability to understand radiative forcing of anthropogenic aerosols, since the uncertainty due to aerosol effects on clouds is exceedingly large [*Charlson et al.*, 1992].

Measurements have demonstrated that aerosol particles can have a strong influence on microphysical and radiative properties of certain clouds. For example, ship effluents often increase the albedo of overlying stratus clouds due to increases in droplet concentration [*Radke et al.*, 1989], and similar effects have been observed downwind of industrial areas [e.g., *Fitzgerald and Spyers-Duran*, 1973; *Twohy et al.*, 1995]. *Leaitch et al.* [1992] compiled data from a series of flights in the northeastern United States and Canada and developed some positive relationships between aerosol number and droplet number. Relationships between CCN number and droplet number have been observed in both stratiform and cumuliform clouds [e.g., *Hudson*, 1983; *Yum et al.*, 1998; *Hudson and Yum*, 2000a]. Some evidence for indirect effects of aerosols on cirrus clouds has even been presented [*Sassen et al.*, 1995].

Thus indirect aerosol effects are recognized as important, but they are still poorly understood. The chemical heterogeneity of the anthropogenic aerosol and its interaction with the background aerosol makes simple parameterizations of questionable validity. Emphasis to date has been on understanding sulfate aerosol effects, but other aerosol types, for example, organics, soil dust, and sea salt, are also likely to be important in cloud formation.

The multinational Indian Ocean Experiment (INDOEX) was designed to study the significance of anthropogenic aerosols to regional and global radiative forcing. During the winter monsoon season in the equatorial Indian Ocean, anthropogenic pollutants from the Northern Hemisphere flow into and interact with pristine Southern Hemispheric air. While much of INDOEX focused on the direct radiative forcing of these pollutants, this work addresses their interaction with clouds. Physical and chemical measurements of aerosols below and within clouds are being used to study the following relationships:

[1]Department of Oceanic and Atmospheric Sciences, Oregon State University, Corvallis, Oregon.
[2]Atmospheric Sciences Division, Desert Research Institute, Reno, Nevada.
[3]Department of Mechanical and Aerospace Engineering, Arizona State University, Tempe, Arizona.
[4]National Center for Atmospheric Research, Boulder, Colorado.
[5]Centro de Ciencias de las Atmosfera, Universidad Nacional Autónoma de Mexico, Ciudad Universitaria, Mexico City, Mexico DF.

Paper number 2000JD900779.
0148-0227/01/2000JD900779$09.00

1.1. Impact of Cloud-Nucleating Aerosol Particles on the Microphysical and Radiative Properties of Clouds

Using satellite observations, clouds in areas of the globe which are polluted have been shown to have smaller droplet sizes and higher albedos than those in less polluted areas [*Han et al.*, 1994; *Wetzel and Stowe*, 1999]. *Han et al.* [1994] observed substantial differences in the low-cloud droplet size inferred from satellite in the INDOEX region, with droplet size increasing downwind of the west coast of India, toward the Equator. In situ observations have also confirmed that increased aerosol concentrations can increase droplet number and decrease droplet size [*Leaitch et al.*, 1992; *Martin et al.*, 1994]. *McFarquhar and Heymsfield* [this issue] and *Heymsfield and McFarquhar* [this issue] verified that aerosol number concentrations were correlated with droplet number and optical depth and anticorrelated with droplet size in the INDOEX region.

The relationship between aerosol number and droplet number varies with location, since it can be affected by particle size and chemical composition, as well as dynamical forcing and entrainment. The relationship is generally thought to be non-linear due to the increased competition for available water among growing droplets in polluted regions. However, droplet concentrations in polluted air may be underestimated in some cases, due to instrumental detection limits [*Bower et al.*, 2000; Hudson, J.G. and S.S. Yum, Spatial distribution of cloud condensation nuclei spectra over the Indian Ocean, submitted to *J. Geophys. Res.*, 2000, hereinafter referred to as Hudson and Yum, submitted manuscript, 2000b].

1.2. Size and Critical Supersaturation of Particles Incorporated Into Droplets

Particles that have a critical supersaturation S_c lower than the supersaturation actually reached within a cloud form activated cloud droplets if given sufficient time for growth [*Squires*, 1952]. Those with higher S_c values will remain as smaller unactivated haze particles within the cloud. S_c is determined by the size and composition of the particle and is related to the number of soluble ions within a particle; larger, more soluble particles will have lower S_cs than smaller, less soluble particles. Simple adiabatic models also predict that the largest droplets in a cloud will form on the largest soluble particles with the lowest S_cs. This relationship can be complicated in clouds in the atmosphere, which are not necessarily adiabatic.

Particles acting as CCN at various supersaturations can be measured by CCN counters or spectrometers that simulate cloud formation under controlled conditions. Comparisons of particle size and S_c can be used to infer information about chemical composition and solubility of ambient and in-cloud aerosol particles.

1.3. Particle Chemical Types Acting As CCN

The ability of naturally soluble sulfate and nitrate particles to act as cloud condensation nuclei is well recognized. However, since elemental carbon and dust particles are often large and can obtain a soluble coating over time [e.g., *DeMott et al.*, 1999; *Dentener et al.*, 1996], they may also be effective CCN. Recent modeling [*O'Dowd et al.*, 1999; *Ghan et al.*, 1998] suggests that in cases of high to moderate wind speeds, the presence of sea salt may dramatically influence the ability of sulfate to affect the microphysical, and therefore the radiative, properties of marine clouds. Organic aerosols can be either water soluble or insoluble depending on their composition [*Facchini et al.*, 1999]. Limited experimental studies suggest that a substantial fraction of organic aerosols can act as cloud condensation nuclei [*Novakov and Penner*, 1993; *Facchini et al.*, 1999]. On the other hand, insoluble or partially soluble organic coatings are likely to have poor nucleating abilities [*Corrigan and Novakov*, 1999].

While models of cloud nucleation and growth are numerous, few measurements of particles actually incorporated into clouds exist. The aerosol plume emanating from India and nearby countries is a complex chemical soup, with sulfate, nitrate, and carbonaceous aerosol from industry mixed with soil dust from desert regions and sea salt from the ocean. INDOEX provided an opportunity to assess interactions of many aerosol types with clouds, both near the heavily polluted source region and over a large region downwind.

2. Experimental Design

During INDOEX, small cumulus and stratocumulus clouds downwind of the Indian sub-continent were sampled by the C-130 aircraft operated by the National Center for Atmospheric Research. The experiment took place during the winter monsoon of February/March of 1999, when the low-level winds were north/northeasterly over the Indian sub-continent and out over the Arabian Sea. Pollutant plumes flowing southwest from the coast of India are readily observable by satellite, and some flights focused on the direct radiative impact of this aerosol. However, a number of flights were devoted to cloud sampling in a concerted effort to detect and quantify the indirect aerosol effect. The C-130 carried a broad range of radiation, aerosol and cloud physics sensors, utilizing both in situ and remote techniques.

Measurements within clouds were made using a counterflow virtual impactor, or CVI [*Ogren et al.*, 1985; *Noone et al.*, 1988]. Within the CVI inlet, cloud droplets larger than about 7 μm diameter were separated from the interstitial aerosol and impacted into dry nitrogen gas. This separation is possible via a counterflow stream of nitrogen out the CVI tip, which very efficiently prevents smaller particles from entering the inlet. The nonvolatile residual nuclei and water vapor remaining after droplet evaporation at 50°C are brought into the aircraft for sampling. Thus, unlike liquid collection techniques, characteristics of individual droplet residual nuclei can be determined. (The particles measured downstream of the CVI inlet after droplet evaporation will be called "residual nuclei" or "droplet nuclei" here for simplicity, although they may contain substances added to the actual cloud droplet nucleus after droplet formation, e.g., through chemical reactions or coalescence. Because particles are typically recycled through clouds many times before their removal from the atmosphere, these particles would also be potential CCN on their next passage through a cloud.) During INDOEX, several different instruments were used downstream of the CVI inlet (Figure 1).

The total number of residual nuclei were measured with a TSI 3760 condensation nucleus counter (CNC), from which the number concentration of sampled droplets was inferred. Water vapor content was measured by a Lyman-α hygrometer, so the liquid water content of the sampled droplets could be determined [e.g., *Twohy et al.*, 1997]. The size distribution of residual nuclei was measured in situ with a PMS 1001

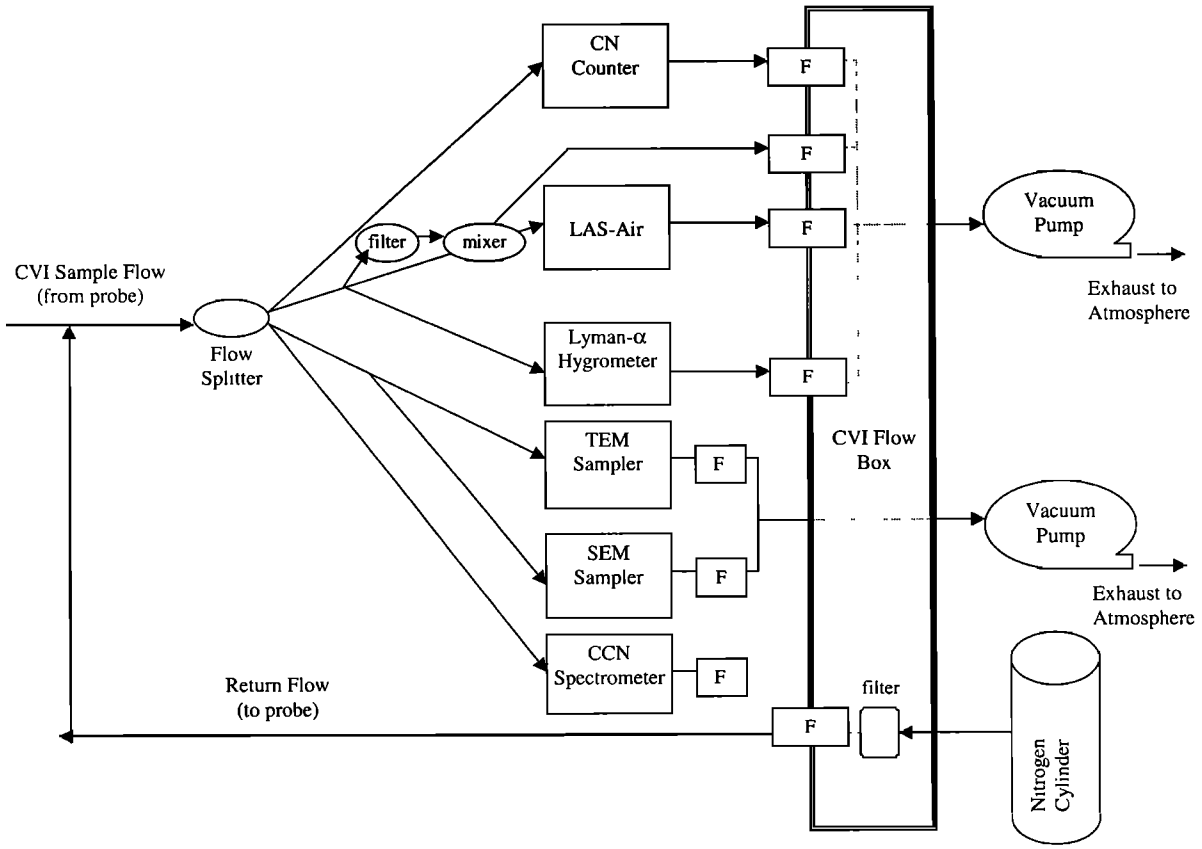

Figure 1. Flow diagram used for sampling with the CVI during INDOEX. The instruments shown in the middle include a condensation nucleus counter, a LAS-Air optical particle counter, a Lyman-α hygrometer, rotating grids for transmission electron microscopy, rotating Nuclepore filters for scanning electron microscopy, and a cloud condensation nucleus spectrometer. "F" denotes a flowmeter or controller.

LAS-Air optical counter, and the actual CCN spectrum (critical supersaturation) of the residual nuclei was determined in situ with a fast-response CCN spectrometer [*Hudson*, 1989; *Twohy and Hudson*, 1995]. Residual nuclei were also collected on filters and impactor grids for later analysis by electron microscopy and X-ray spectrometry [*Anderson et al.*, 1996].

3. Analysis

One challenge in the analysis and interpretation of this data set was the relatively small scale of the INDOEX clouds: most clouds encountered were only 0.3 to 1 km wide and of similar depth. In order to get sufficient residual nuclei samples for chemical analysis, the data presented here have been averaged over many cloud passes. As a result, characteristics of cloud parcels with many different histories, including cloud edges, have been included in the results. This means that the data are far from representative of a simple, adiabatic cloud. In addition, sampling considerations limit the size of droplets that were effectively sampled by the CVI to those larger than about 7 μm in diameter. In very polluted clouds, the mean droplet diameter was sometimes 7 μm or smaller, so that a fraction of the droplets could not be sampled by the CVI. Clouds containing drizzle drops, which can produce artificial particles due to drop breakup within the inlet, have been excluded from this analysis. Despite these limitations, useful information was obtained using the analysis strategies outlined below.

For each analysis type, characteristics of the droplet nuclei were compared with corresponding characteristics of the below-cloud aerosol. Cases defined as clean or polluted were compared and contrasted.

3.1. Particle Size Distributions

Size distributions of the ambient aerosol and CVI residual nuclei were constructed using data from the LAS-Air optical particle counter (0.1 to 4.0 μm diameter) and TSI condensation nucleus counter (> 0.013 μm diameter). Since the CNC samples smaller particles as well as large ones, a nine-channel size distribution was constructed using the eight LAS-Air channels and the CN concentration minus the total LAS-Air concentration for the smallest size channel. To avoid excessive width in the lowest channel of the size distribution, it was assumed to begin at 0.03 microns diameter. This is consistent with the rarity of particles less than 0.03 μm and the typical lower limit of size distributions in the study area (A. D. Clarke, unpublished data, 2000).

Since the CVI tip is heated and droplets are impacted into dry nitrogen gas, the relative humidity of the size distributions presented here was generally less than 20% and the particles are considered to be "dry." Droplet concentrations are enhanced within the CVI, so a dilution system was employed to avoid coincidence (multiple particles in the sensing volume)

in the LAS-Air. Data were initially corrected for both enhancement and subsequent dilution. The time resolution of the LAS-Air is 6 s, but several minutes were averaged for the data presented here in order to match the sampling periods required for electron microscopy. Since only a fraction of this time contained cloud passes, the CVI data were also divided by a "time in cloud" factor, TIC. TIC was calculated as the ratio of the number of seconds in cloud divided by the number of seconds in the entire sampling period. Clouds were defined as events of >0.3 km in length when the droplet concentration from the wing-mounted Forward Scattering Spectrometer Probe (FSSP) was greater than 10 cm^{-3}.

Ambient below-cloud aerosol was also measured with the LAS-Air, using the CVI inlet with the counterflow turned off. Since sampling under these conditions is subisokinetic, corrections were applied as a function of particle size based on *Belyaev and Levin* [1974]. Because of uncertainties in the coincidence correction, dilution factors, and instrument response to various particle types [*Pinnick et al.*, 2000], the overall uncertainty in both particle size and concentration is estimated at about 20%.

3.2. Aerosol Critical Supersaturations From CCN Spectrometer

Complete CCN spectra (number concentrations at S_cs from 0.01 to 1.0%) were obtained for droplet nuclei using the CVI and for corresponding below-cloud samples brought in through the Community Aerosol Inlet (CAI). Collection efficiency of the CAI for submicron particles is near 100% [*Blomquist et al.*, 2000], and particles larger than 1 micron are expected to have S_cs less than 0.01%. Although inversion corrections have been recently implemented to the CCN spectra (Hudson and Yum, submitted manuscript, 2000b) these corrections are not expected to substantially change the integrated CCN number concentrations or median critical supersaturations presented here. As a result, no special corrections were applied.

While the time response of the DRI CCN spectrometer is as fast as 1 Hz, data have been averaged over the same time periods as the EM samples whenever possible to facilitate direct comparison of results. For ease of comparison, summary parameters, specifically CCN number concentration and median S_c, are presented here. These summary parameters are used to contrast clean and polluted cases and to compare with similar parameters from other instruments.

3.3. Particle Composition via SEM/TEM

Droplet residual nuclei were simultaneously collected for both SEM and TEM behind the CVI. Automated SEM analysis with energy-dispersive X-ray spectroscopy [*Anderson et al.*, 1996] provides size-dependent single-particle composition for several particle types, including sea salt, sulfates, and soil dust. This technique also produces information on the mixing state of particles (i.e., whether different chemical species are present within single particles, or separate particles). More detailed structural information, especially about carbonaceous aerosols, can be obtained via TEM with energy-dispersive spectrometry [*Posfai et al.*, 1995]. This type of analysis is critical in determining what particle types actually participate in cloud formation. For example, using the CVI and TEM, *Twohy and Gandrud* [1998] found that both mineral and metallic particles apparently can form ice crystals in aircraft contrails, although these particle types were previously considered to be relatively unimportant. Since this analysis is ongoing and will be detailed in a subsequent paper, initial SEM results are only briefly discussed here.

3.4. Case Studies

Four cases were chosen for detailed analysis, ranging from clean to very polluted environments. While clouds were sampled on several other days, these cases provided the most extensive data in nonprecipitating clouds and the most comprehensive array of measurements (chemical, microphysical, and radiative).

Pollution levels were defined following *McFarquhar and Heymsfield* [this issue] and are based on the ambient measurements of total condensation nuclei (CN). Number concentrations <500 cm^{-3} were considered clean and >1500 cm^{-3} polluted, recognizing that cases with CN between 300 cm^{-3} and 500 cm^{-3} may have actually had some anthropogenic influence. (Pristine marine environments have typical CN concentrations on order 200-300 cm^{-3} [*Gras*, 1995].) Regions exhibiting ultrafine particle production were rare and were not included in this analysis.

Concentrations of CN and chemical species such as non-sea salt sulfate, black carbon and organic carbon were well correlated with distance downwind of the Indian coastline [*Satheesh et al.*, 1998; *Cantrell et al.*, 2000; *Guazzotti et al.*, 2000], with more northerly latitudes generally having higher pollution levels. For reference, the southern tip of India is at about 8°N latitude. Clean flights were south of the Intertropical Convergence Zone (ITCZ) in the Southern Hemisphere, while polluted flights were over the ocean, west of India.

The first case (March 24, 1999, 6°-7°S) exhibited among the cleanest air and clouds encountered during the INDOEX experiment. Since nearly all droplets were larger than the CVI cut size (7.2 μm diameter in this case), overall droplet collection efficiency was high at the minimum cut size. The second clean case (February 20, 1999, 6°-7°S) was in a similar geographical location, but with slightly higher particle number concentrations. The third and fourth cases (March 21, 1999, 10°-11°N; February 27, 1999, 8°-9°N) were both polluted, but the dynamical forcing was greater in the fourth case. This led to larger droplets and liquid water contents, so a greater fraction of droplets could be sampled by the CVI.

4. Results

4.1. Summary of Statistics for Four Cases

A summary of aerosol and cloud characteristics for the four cases is given in Table 1. The cases are ordered from low to high pollution levels. Statistics for each row represent averages for between 6 and 46 individual cloud passes, but there was considerable variation from cloud to cloud. Ambient samples were taken at various heights below cloud base. The CVI cut size, or size of droplet collected with 50% efficiency, is also given [*Anderson et al.*, 1993]. For two of the cases, CVI samples were obtained at both a minimum and a larger droplet cut size.

Maximum updrafts were near 1.0 m s^{-1}, and up to 1.4 m s^{-1} for the most vigorous case on 27 February. Since most clouds were only a few hundred meters in horizontal extent, many cloud edges were sampled, and mean updrafts were considerably lower (approximately 0.3 m s^{-1}). Cloud droplet concen-

Table 1. Summary of Selected Cloud Characteristics[a]

	Date	UTC Time	Cloud					Aerosol				
			Updraft, $m\ s^{-1}$ maximum	N_{drop}, cm^{-3} mean	N_{drop}, cm^{-3} maximum	LWC, $g\ m^{-3}$ mean	MVD, μm mean	N_{CN}, cm^{-3} mean	N_{CN}, % of N_{drop} mean	N_{CCN}, cm^{-3} mean	S_c, % median	D_p, μm median
CLEAN	March 24, 1999											
Ambient aerosol		0853-0924	-	-	-	-	-	207	-	153	0.135	0.11
Cloud A		0821-0835	0.85	56	95	0.089	16.6					
Cloud B		0847-0851	1.1	47	87	0.085	17.0					
CVI A: >7.2 μm		0821-0835						63	112%		0.11	0.092
CVI B: >12.8 μm		0847-0851						12	26%		0.105	0.155
CLEAN	Feb. 20, 1999											
Ambient aerosol		0538-0541	-	-	-	-	-	338	-	204	0.15	0.11
Cloud		0601-0623	1.01	116	198	0.093	15.0					
CVI: >7.8 μm		0601-0623						84	72%		0.15	0.082
POLLUTED	March 21, 1999											
Ambient aerosol		0828-0840	-	-	-	-	-	1601	-	1043	0.17	0.092
Cloud A		0800-0825	0.90	137	239	0.060	11.9					
Cloud B		0750-0800	0.75	122	228	0.040	11.6					
CVI A: >7.0 μm		0800-0825						46	34%		0.073	0.20
CVI B: >8.2 μm		0750-0800						12	10%		0.040	0.255
POLLUTED	Feb. 27, 1999											
Ambient aerosol		0803-0813	-	-	-	-	-	2002	-	1752	0.225	0.089
Cloud		0726-0800	1.4	167	306	0.12	13.9					
CVI: >7.2 μm		0726-0800						122	73%		0.037	0.15

[a]Data pertaining to ambient aerosol, cloud, and CVI measurements are given in separate rows for each case. For cloud and CVI data each value represents average properties of a number (between 6 and 46) of individual cloud passes at constant altitude. When two CVI cut sizes were used sequentially, legs have been denoted A and B, respectively. N_{drop} is number concentration from FSSP-100, LWC is cloud liquid water content from the 1st King Probe (PLWCC), MVD is median volume diameter from the FSSP. CN concentrations (N_{CN}) are from the CVI CN counter which sampled both ambient and cloud residual nuclei concentrations; % of N_{drop} refers to CVI residual nuclei concentration relative to FSSP droplet concentration in percent. N_{CCN} and S_c data are from the DRI CCN spectrometer and represent particles with critical supersaturations S_c of up to 1.0%. D_p is the dry diameter derived from the CVI LAS-Air and CNC. Since both S_c and D_p are spectral parameters, median values of the spectrum are given.

trations (N_{drop}) were generally low, even for the polluted clouds. While coalescence (in the clean clouds) and poor cloud-nucleating qualities of the aerosol (in the polluted clouds) may be partially responsible, Hudson and Yum (submitted manuscript, 2000b) found that on average, liquid water contents were less than 20% of the adiabatic value in both cloud types. Substantial evaporation of droplets apparently occurred during the clouds' lifetimes, with measured droplet concentrations significantly reduced from adiabatic values. Despite this, droplet concentrations are positively correlated with particle concentrations (both N_{CN} and N_{CCN}). For the cleaner clouds, maximum droplet concentrations are 50-60% of the available particle number concentrations, while for the polluted clouds, this percentage is only about 15%. Corresponding percentages using mean droplet concentrations are only about 25-35% and 5-10%. Further relationships of this type using more observations are given by Hudson and Yum (submitted manuscript, 2000b) and *Heymsfield and McFarquhar* [this issue].

Droplet sizes are smaller for the polluted cases, as predicted by *Twomey* [1977a] and observed by *McFarquhar and Heymsfield* [this issue]. However, the influence of dynamics is apparent in the characteristics of the most polluted case (February 27). These clouds had relatively large updraft velocities and liquid water contents, so the droplets were substantially larger than for the other polluted case.

For the rows displaying CVI measurements, N_{CN} is the mean number of droplet nuclei sampled; the percent of N_{drop} category shows this percentage relative to the total droplet number concentration measured by the FSSP-100. Percentages larger than 100 occasionally occurred due to instrumental uncertainty and different portions of the clouds being sampled by the instruments mounted in different areas of the aircraft. Most of the droplets in these clouds were large enough to be collected by the CVI, with percentages relative to the FSSP of 70% or greater. In the third case, however, the droplets were so small that many were below the minimum cut size of about 7 μm diameter, but were still detected by the FSSP, with a minimum size of 2 μm. (Note the droplet diameters given in the table are median volume diameters, not mean diameters, which were much smaller.)

Both critical supersaturation and particle size measurements were made over a range of values, so the median values for the ambient aerosol and droplet nuclei are given in the last two columns of Table 1. Peak cloud supersaturations were likely much higher than the median S_c of the droplet nuclei given in the table. Minor differences between ambient and nuclei properties are apparent in the first clean case, with droplet nuclei having slightly lower S_cs than the ambient aerosol. Median sizes, however, are actually smaller for the droplet nuclei than for the ambient aerosol in both clean cases, in contrast with simple theory. This suggests that insoluble material that may have inhibited activation was present in certain particle sizes. This is supported by the size distributions given in the next section. By far the largest differences between ambient and nuclei properties, however, occur in the polluted clouds. For these cases, droplet nuclei tend to be much larger and to have much lower critical supersaturations compared to the ambient aerosol. This is true even for the February 27 case, when most of the droplets, not just the upper "tail" of the distribution, were sampled by the CVI. Reasons for this are discussed subsequently.

4.2. Size Distributions

Figures 2 and 3 compare the measured ambient and nuclei size distributions for the clean and polluted cases, respectively. Distributions have been plotted with both linear and logarithmic ordinate axes to focus on different details of the distribution. Ambient size distributions are represented with heavy solid lines, and droplet nuclei distributions with dashed lines. Since the polluted aerosol was already substantially aged, bimodal ambient distributions that may have been a result of in-cloud chemical reactions (last row of Figure 3) were not uncommon. The far right panes show the percentage of ambient particles in each size range that were found within droplets sampled by the CVI. While the distributions are rather coarse, several important observations can be made.

First, it is apparent that the number of residual nuclei is substantially smaller than the number of available particles, even for the clean cases shown in Figure 2. Since the modeling results given in the next section indicate that nearly all particles are expected to form droplets in a clean cloud, cloud processes subsequent to droplet formation are the likely cause of this apparent discrepancy. Entrainment of droplet-free air into the cloud would reduce the droplet number concentration through dilution and evaporation in both the clean and polluted clouds. Coalescence could also act to reduce the number concentration in clean clouds, but would be less efficient in the polluted clouds, due to the small droplet sizes. However, droplet nucleation and growth is expected to be less efficient in polluted clouds due to lower peak supersaturations (see modeling section).

The shape of the relative distribution in the final pane is fairly regular for the polluted clouds (Figure 3), and shows progressively more involvement of the larger particles in the drops. Note that relatively few particles in the smallest size categories are incorporated into the polluted clouds. This is to be expected from cloud nucleation theory, since larger particles generally have greater amounts of soluble material and lower critical supersaturations; these are the ones expected to preferentially form cloud droplets if available water is limited. Mixing of noncloudy air in individual clouds, as well as mixing of cloud parcels with different histories in a single sample, will produce the stepwise distribution shown in Figure 3. Also, in-cloud chemical reactions could shift particles into larger size channels.

The shape of the relative distributions for the clean clouds (Figure 2) is more complex. Nearly all particles in the clean regions are expected to form droplets, and these plots do show that a higher percentage of small particles are incorporated into these clouds relative to polluted clouds. However, the plots indicate a relative deficit of intermediate-sized particles, particularly between 0.2 and 0.3 microns in diameter. This may have been due to size-dependent composition of the ambient aerosol, with some less soluble particle type (perhaps surviving convection in the ITCZ) in this size range. There is also a relative enhancement of large cloud nuclei within the clean cloud droplets, with percentages larger than 100%. Coalescence will decrease the number of small and intermediate-sized nuclei and will enhance the number of large residuals [e.g., *Ogren and Charlson*, 1992]. This process is expected to be more prevalent in the clean clouds with larger droplets. Also, some particle aggregation was apparent in the electron microscope analysis of residual nuclei for the clean clouds, perhaps as a consequence of droplet coalescence.

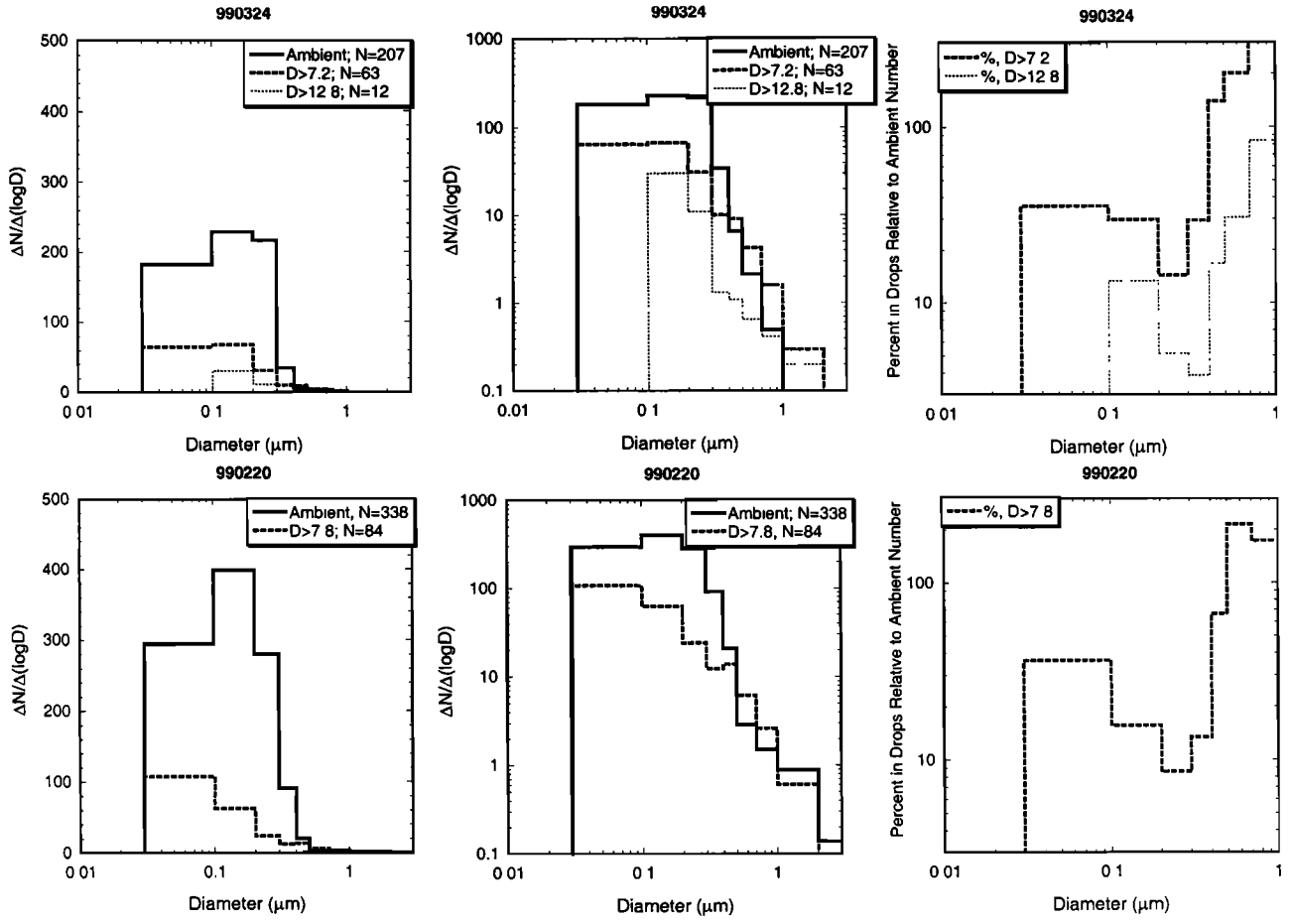

Figure 2. Comparison of aerosol size distributions measured below cloud and with the CVI for clean cases on March 24, 1999 (top row) and February 20, 1999 (lower row). Ambient size distributions are represented with heavy solid lines, and droplet nuclei are shown with dashed lines. The first pane in each row shows the size distribution with a linear ordinate axis, with the area within the histogram proportional to the actual particle number. The second pane shows the distribution with a logarithmic ordinate axis for more detail. The far right panes show the percentage of ambient particles in each size range that were found within droplets sampled by the CVI. These panes have been truncated at 1.0 μm diameter due to poor counting statistics at the large particle sizes.

4.3. Model Calculations

The above results suggest several important differences in clean and polluted clouds, some of which have been studied using simple model calculations. Three cases were simulated in order to highlight potential differences in particle activation in clean and polluted clouds. The Model for Aerosol Process Studies (MAPS), based on a detailed aerosol model developed by *Wexler et al.* [1994], has been expanded to include cloud formation. Also, it has recently been tested against other models at a World Meteorological Organization workshop, and improved based on these results.

The first ("Clean") case, based on the March 24 flight, was initiated using the below-cloud temperature, pressure, and relative humidity, with a lognormal fit to the aerosol size distribution measured at 310 m. Sixty-four size bins were used in the lognormal distribution with a geometric mean diameter of 0.115 μm, a geometric standard deviation of 1.77, and a total number concentration of 207.6 cm^{-3} (dry aerosol mass equal to 1.29 μg m^{-3}). The updraft velocity was 0.3 m s^{-1}, the average for all cloud penetrations during this sampling period. Simulations were terminated at 600 m altitude, where the in-cloud measurements were made. For the second ("Polluted A") case, the same aerosol size distribution and atmospheric conditions were used, but the total number concentration was increased by a factor of 10 to 2076 cm^{-3} (dry aerosol mass equal to 12.9 μg m^{-3}). For the first two simulations, all particles were composed simply of ammonium bisulfate, and no condensing species other than water vapor was considered. While the presence of soluble gases and slightly soluble aerosol species can affect droplet activation [e.g., *Laaksonen et al.*, 1998], this simple scenario has been used to emphasize differences due to number concentration alone, and the sense of the results will apply to any soluble particle type. Also, MAPS calculates particle growth kinetically, so particles are not assumed to immediately activate when the cloud supersaturation exceeds their critical supersaturation.

For the final simulation ("Polluted B"), the same size distribution was used as in the Polluted A case, but particles were assumed to contain an insoluble elemental carbon core surrounded by ammonium bisulfate. The volume of ammonium bisulfate (density 1.78 g cm^{-3}) was 60% of the total particle volume, in accordance with some measured soluble vol-

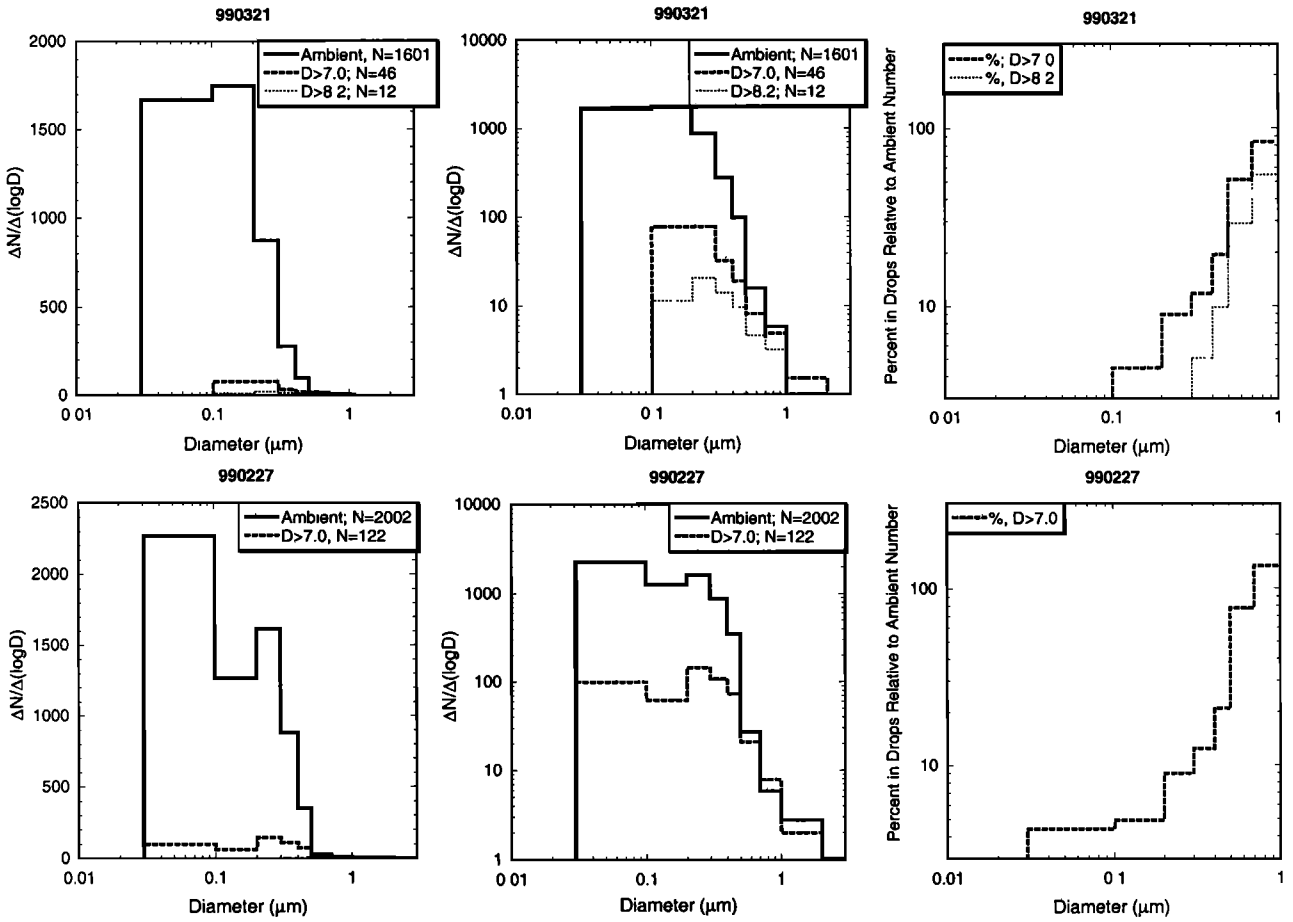

Figure 3. As in Figure 2, but for polluted cases on March 21, 1999 (top row) and February 27, 1999 (lower row).

ume fractions for polluted INDOEX aerosol [*Massling et al.*, 2000]. Elemental carbon was assumed to have the same density as ammonium bisulfate, so that the soluble mass fraction was also 60%. Of course, more complex particle types (including external mixtures), different size distributions, soluble gases, and in-cloud processes and chemical reactions can also affect how particles are incorporated into cloud. Simulations of these types are planned for future work.

Table 2 shows the primary differences in results for the three cases. In all cases, the in-cloud supersaturation peaks just above cloud base, but subsequently decreases as water vapor is depleted by rapidly growing droplets. The peak supersaturation reaches 0.33% in the Clean case, but only 0.17% in the Polluted A case and 0.20% in the Polluted B case, since water condenses on a greater number of particles. The S_c of certain particles is exceeded only briefly, and they do not necessarily grow into droplets due to kinetic limitations. However, at the end of the simulations, a clear separation occurs between larger droplets and smaller particles, and a particle was considered to be "activated" if it was contained in the larger mode at the end of the simulation.

Because of the difference in peak supersaturation, much smaller particles activate in the Clean case than in the Polluted cases (down to 0.068 μm for Clean versus 0.123 or 0.131 μm for Polluted). The percent of particles activated is 84% in the clean case, and only 48% and 43% in the Polluted A and B cases, respectively. This effect has been discussed by *Twomey* [1977a] and others. Also note that the S_c of the minimum particle size activated is significantly less than the peak cloud supersaturation in all three cases, due to kinetic limitations on growth.

The median critical supersaturation and diameter of ambient and activated ("cloud") particles is also given in Table 2. For the Clean case these values can be compared directly to the measured values for March 24 in the last two columns of Table 1. The median S_cs predicted by the model and the measurements agree well within the experimental uncertainty (0.132 versus 0.135 for ambient particles and 0.112 versus

Table 2. Summary of Cloud Model Results[a]

	Clean 100% Soluble	Polluted A 100% Soluble	Polluted B 60% Soluble
N_p, cm^{-3}	207.6	2076	2076
Peak cloud S, %	0.33	0.17	0.20
N_p activated	175	998	903
Percent of N_p activated	84%	48%	43%
Min D_p activated, μm	0.068	0.123	0.131
S_c of min D_p activated	0.276	0.116	0.136
Ambient D_p, μm (med)	0.112	0.112	0.112
Ambient S_c, % (med)	0.132	0.132	0.173
Cloud D_p, μm (med)	0.125	0.168	0.175
Cloud S_c, % (med)	0.111	0.073	0.089

[a]Summary of results for three model cases discussed in text. All diameters refer to dry particle sizes. S is supersaturation; S_c is critical supersaturation.

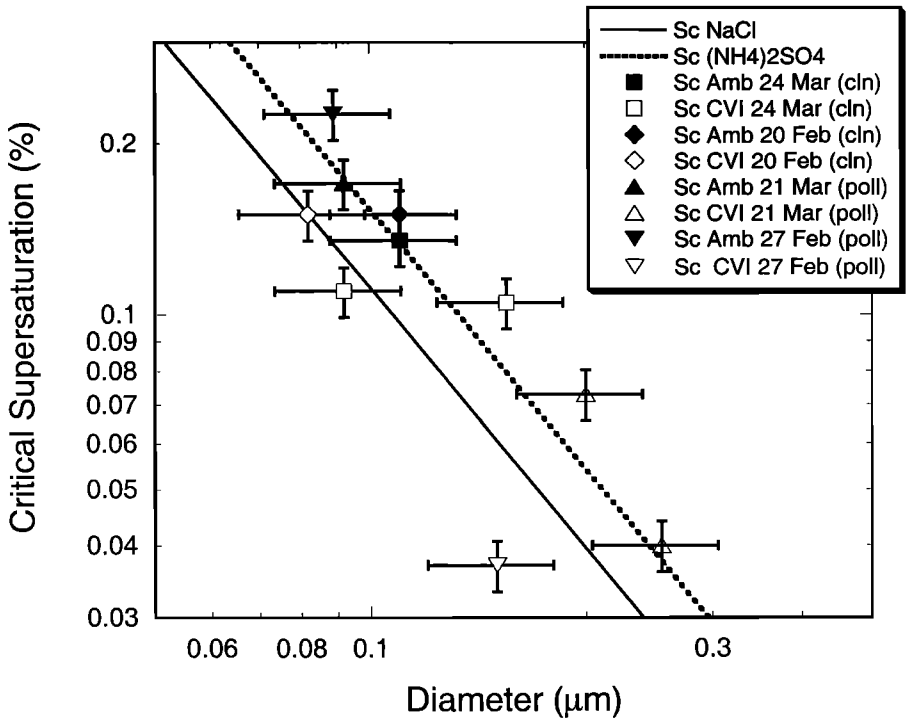

Figure 4. Dry particle diameter versus critical supersaturation (S_c) for NaCl (solid line) and $(NH_4)_2SO_4$ (dashed line) from *Twomey* [1977b]. Median diameters for both ambient (solid symbols) and CVI measurements (open symbols) using the LAS-Air particle counter are compared with median critical supersaturations from the CCN spectrometer. Clean cases have square and diamond symbols, and polluted cases have triangular symbols. Uncertainty (error bar) values are estimated at 20% for diameter and 10% for S_c.

0.11 for activated particles). The median diameter for activated particles predicted by the model is larger than the measurement (0.125 versus 0.092). As discussed earlier, this may represent the influence of some other, less soluble particle type in the ambient aerosol that is less likely to activate. For the polluted cases, large differences in both the median particle size and S_c occur between the ambient and activated particles. These differences agree qualitatively with the measurements for polluted clouds having different initial particle size distributions (Table 1).

To summarize, higher particle number concentrations in polluted air have a strong influence on the fraction of particles that activate and whether small, high S_c particles will be incorporated into clouds. Insoluble material that may be contained in polluted particles seems to have a secondary and complementary effect, further reducing the percentage of particles that activate and the distinction between ambient and activated particle size.

4.4. S_c Versus Size

In Figure 4, median diameters for both ambient and CVI measurements using the LAS-Air particle counter are compared with median critical supersaturations from the CCN spectrometer. For reference, S_c values expected for NaCl (molecular weight 58.5) and $(NH_4)_2SO_4$ (molecular weight 132) are shown with solid and dashed lines, respectively. Ammonium bisulfate (115) would fall between these two lines. For consistency with the calibration procedure for the CCN spectrometer, complete ionic dissociation following *Twomey* [1977b] has been assumed. Nonideal effects reduce the amount of ionic dissociation and raise the S_c [*Chylek and Wong*, 1998], but should not affect the relative differences presented in the figure (since both the theory and measurements use the Twomey formulation for S_c).

The size and S_c values are clearly anticorrelated, and the slope of the data is similar to that expected for simple soluble salts. As was apparent in Table 1, the CVI samples (hollow symbols) tend to lower S_cs and larger sizes than the ambient samples. While some of the CVI samples exhibit characteristics similar to sodium chloride, many of the data points have higher S_cs than those expected for sodium chloride, ammonium bisulfate, or ammonium sulfate. The presence of insoluble material (elemental carbon, crustal material, or sparingly soluble organics) could explain these results, as could mixed salts or soluble material with more ions per molecule or a greater molecular weight.

The median size and critical supersaturations have been used to estimate the soluble mass fraction, ε, for each of these samples following *Cantrell et al.* [2000]. For simplicity, these calculations assume that particles are internal mixtures of ammonium sulfate and some insoluble material. However, partially soluble materials or coatings would also influence S_c and, therefore, calculated ε values. Results have large uncertainties, but are included here for comparison with other estimates for the INDOEX region. *Cantrell et al.* [2000] inferred soluble fractions in the ambient aerosol as low as 0.20 south of the ITCZ and values around 0.05 north of the ITCZ in 1998, but found higher values in 1999 (W. Cantrell, personal communication, 2000). *Massling et al.* [2000] measured soluble volume fractions more directly using tandem differential mobility analyzers and found higher soluble fractions in 1999, generally between 0.60 and greater than 1.0 for 0.15 μm par-

Table 3. Inferred Particle Solubilities[a]

	Date	UTC Time	S_c, % median	D_p, μm median	Soluble Fraction (and Range based on Uncertainty)	Soluble Volume, μm^3	Solubility Ratio (CVI/Ambient)
CLEAN	March 24, 1999						
Ambient aerosol		0853-0924	0.135	0.11	0.96 (0.66-1.5)	0.0054	-
CVI A: >7.2 μm		0821-0835	0.11	0.092	2.5 (1.7-3.8)	0.0081	1.5
CVI B: >12.8 μm		0847-0851	0.105	0.155	0.57 (0.39-0.87)	0.0089	1.6
CLEAN	Feb. 20, 1999						
Ambient aerosol		0538-0541	0.15	0.11	0.78 (0.53-1.2)	0.0044	-
CVI: >7.8 μm		0601-0623	0.15	0.082	1.9 (1.3-2.9)	0.0044	1.0
POLLUTED	March 21, 1999						
Ambient aerosol		0828-0840	0.17	0.092	1.0 (0.71-1.6)	0.0034	-
CVI A: >7.0 μm		0800-0825	0.073	0.20	0.55 (0.37-0.83)	0.018	5.3
CVI B: >8.2 μm		0750-0800	0.040	0.255	0.88 (0.60-1.3)	0.061	18
POLLUTED	Feb. 27, 1999						
Ambient aerosol		0803-0813	0.225	0.089	0.66 (0.45-1.0)	0.0019	-
CVI: >7.2 μm		0726-0800	0.037	0.15	5.1 (3.4-7.7)	0.072	38

[a]As in Table 1, with the addition of particle soluble mass fraction inferred from the median S_c and dry particle diameter. Soluble fractions were calculated as discussed in the text, and soluble volume amounts (per particle) were calculated from soluble mass fractions and median diameters, assuming the same density for soluble and insoluble material. Solubility ratios are the soluble volume amounts (per particle) for the CVI residual nuclei divided by the soluble volume amounts for the ambient aerosol.

ticles (based on ammonium sulfate or bisulfate). Some less hygroscopic particles were found, however, even in relatively clean air masses south of the ITCZ. *Cantrell et al.* [2000] suggest that interhemispheric transport, with selective removal of soluble material by convective clouds in the ITCZ, may impose an insoluble aerosol component into the Southern Hemisphere air.

Inferred particle solubilities are given in Table 3, both as soluble mass fractions and as total volume of soluble material (assuming similar densities of soluble and insoluble material). Soluble fractions range from 0.66 to 1.0 for the ambient samples, in approximate agreement with *Massling et al.* [2000]. This indicates consistency between the measured size distributions and CCN spectra and the expected composition of the aerosol. While no clear difference between solubility for the clean versus polluted samples is apparent, a range of solubilities is expected in both clean and polluted air masses [*Massling et al.*, 2000]. Also, large uncertainties mean that differences on order 30% may not be significant.

The CVI samples exhibit a wide range of soluble fractions, ranging from as low as 0.55 to as high as 5.1. Fractions larger than 1.0 are common for the droplet nuclei and indicate a substance with higher S_c than ammonium sulfate for the same particle size; for example, NaCl would have an ε of 1.87 using this technique. The value of 5.1 is probably artificially high, due to a large uncertainty in the CCN measurements at very low S_c [*Nenes et al.*, 2000]. Relatively low soluble fractions are also found for some of the CVI samples, which can be explained when the total soluble volume per particle (2nd to last column) is calculated. Low ε values in the first and third cases are compensated for by the larger size of the droplet nuclei, so that the total volume of soluble material is still greater for the CVI samples than for the ambient particles. This indicates that even relatively insoluble particles can be incorporated into clouds if they are sufficiently large. Size or composition measurements alone are therefore insufficient to predict cloud-nucleating properties. Both size and detailed composition information, or direct measurements of CCN, are required.

The last column in Table 3 shows the ratio of soluble volume per particle in the CVI versus ambient particles. For the clean cases, ratios are near one, while for the polluted cases, they greatly exceed one. This supports the differences observed in S_c and indicates that in the clean cases, most particles form droplets. In the polluted cases, however, only a subset of particles, those with more total soluble material, form droplets. This is primarily due to the higher number concentrations in polluted regions which reduce the peak cloud supersaturation, as described in the modeling section. Very high solubility ratios of CVI to ambient as shown in the last case could also occur due to aqueous-phase sulfate production, which is more likely to occur in polluted air masses.

4.5. Electron Microscopy

Electron microscope analysis is not yet complete, and is only briefly discussed here. Early results show a high percentage of submicron sea salt in the cloud samples relative to the ambient aerosol. *Satheesh et al.* [1998] observed that the contribution of sea salt to the total aerosol could be substantial, even in the polluted Indian Ocean. During the 1999 INDOEX experiment, sea salt mass concentrations were generally low relative to the total aerosol. However, submicron sea salt was apparently one of the dominant cloud-nucleating aerosol types. Because of their high solubility, low molecular weight, and relatively large size, sea salt particles are superb cloud condensation nuclei. They are better CCN than the same-sized sulfate particle (Figure 4), and their presence is expect to affect activation of sulfate aerosol [*O'Dowd et al.*, 1999]. In addition, they will react chemically and form internally mixed particles with sulfate [e.g., *Twohy et al.*, 1989; *O'Dowd et al.*, 1999]. This is expected to limit the tendency of sulfate to form new aerosol particles, potentially reducing the indirect effect of anthropogenic sulfur emissions [*O'Dowd et al.*, 1999].

As mentioned earlier, clean samples show significant particle aggregation, perhaps due to droplet coalescence. Also, some unidentified particle types, apparently carbonaceous, were observed even in the "clean" ambient samples. This is

consistent with particle size distributions for the clean droplet nuclei, which suggest some particle types with intermediate sizes are less effective CCN. Since more coal and biomass is burned in Asia than in Europe and North America, large quantities of carbonaceous aerosols (both elemental carbon, EC, and more complex organic species, OC) are produced. While particles with no detectable signatures, assumed to be carbonaceous, and combustion-derived particles are observed in the cloud samples, they are more common in the ambient samples. Additionally, TEM observations indicate that ambient sulfate particles may be coated with carbonaceous material in polluted environments.

4.6. Future Work

Completion of the electron microscope analysis is essential, since all of the results discussed here could be expanded with better knowledge of the chemical composition of both the ambient particles and droplet nuclei. Integration with chemical information from other investigators will also be useful. With detailed chemical information, modeling efforts will be expanded to study the effects of different particle types on cloud formation, and more complex cloud processes, including chemical reactions, can be added. Since the MAPS model was originally designed for polluted situations and includes organic chemistry, effects of various carbonaceous aerosol types can be assessed. Finally, focused experiments in more uniform cloud fields (stratus/stratocumulus) would be useful.

5. Summary and Conclusions

Two clean and two polluted case studies of small clouds in the Indian Ocean region were described. Droplets were collected, evaporated, and their residual nuclei compared with the below-cloud aerosol to determine which of the ambient aerosol act as droplet nuclei under different conditions. The following results are based on these data and simple modeling studies:

1. Droplet concentrations were correlated with particle and CCN concentrations, but a higher fraction of particles formed droplets in the clean cases. While droplet sizes tended to be smaller in the polluted clouds, dynamical forcing (updraft velocity) also impacted droplet size. Entrainment and mixing with dry air was important in reducing the droplet number concentration in both clean and polluted clouds.

2. In the clean clouds the median properties (critical supersaturation and dry size) of the ambient below-cloud aerosol and droplet nuclei were similar. This suggests that most particles were potential nuclei and that a high fraction actually produced droplets. Even particles smaller than 0.1 μm diameter were found to be droplet nuclei in clean clouds. However, some evidence of a less soluble aerosol type was found. In polluted clouds there were stronger differences between ambient aerosol and droplet nuclei, with the larger, lower S_c particles preferentially incorporated into drops.

3. Model simulations were used to show that in polluted regions with high particle number concentrations, lower peak supersaturations are expected. Therefore small and/or mostly insoluble particles with high S_c are much less likely to form droplets in polluted regions than in clean regions. This means that many anthropogenic particles will not participate in cloud formation, and that only the low S_c particles will be important to the indirect effect. These model results were confirmed by the INDOEX data.

4. The median measured critical supersaturation and particle size was used to estimate the particle soluble fraction, assuming ammonium sulfate. Soluble fractions of 0.66 to 1.0 for the ambient aerosol agreed with some other studies in the INDOEX region. For droplet nuclei, soluble fractions could be lower or higher than this. The total amount of soluble material per particle, however, was more informative, and was similar for the ambient particles and droplet nuclei in the clean cases. For the polluted cases, droplet nuclei contained much more soluble material than the ambient samples (based on median values), indicating again that only selected particles act as nuclei in polluted clouds.

5. Early electron microscope results confirm the importance of sea salt (which is a better CCN than ammonium sulfate or bisulfate for the same particle size) in droplet formation. They also suggest that at least some carbonaceous particles are incorporated into clouds. The EM analysis is ongoing, and will provide additional information on composition and mixing states of both ambient and droplet nuclei.

Acknowledgments. This work was primarily supported by the National Science Foundation through grant ATM-9906903, with additional support from the Atmospheric Technology Division at the National Center for Atmospheric Research. We wish to thank the operations and support crew of the NCAR C-130 aircraft, Mr. Errol Korn of NCAR, and two anonymous reviewers who provided useful comments.

References

Albrecht, B.A., Aerosols, cloud microphysics, and fractional cloudiness, *Science, 245*, 1227-1230, 1989.

Anderson, J.R., P.R Buseck and R. Arimoto, Characterization of the Bermuda Aerosol by combined individual-particle and bulk-aerosol analysis, *Atmos. Environ. 30*, 319-338, 1996.

Anderson, T.L., R.J. Charlson, and D.S. Covert, Calibration of a counterflow virtual impactor at aerodynamic diameters from 1 to 15 μm, *Aerosol Sci. Technol., 19*, 317-329, 1993.

Belyaev, S. P., and L. M. Levin, Techniques for collection of representative aerosol samples, *J. Aerosol Sci., 5*, 325-338, 1974.

Blomquist, B.W., B.J. Huebert, S.G. Howell, M. Litchy, C.H. Twohy, A. Schanot, D. Baumgardner, B. Lafleur, R. Seebaugh, and M.L. Laucks, An evaluation of the community aerosol inlet for the NCAR C-130, *J. Atmos. Ocean. Technol.* in press, 2000.

Bower, K. N., T.W. Choularton, and D.E. Sherman, An overview of the ACE-2 ground-based cloud experiment, *Tellus, Ser. B, 52*, 750-778, 2000.

Cantrell, W., G. Shaw, C. Leck, L. Granat, and H. Cachier, Relationships between cloud condensation nuclei spectra and aerosol particles on a south-north transect of the Indian Ocean, *J. Geophys. Res., 105*, 15,313-15,320, 2000.

Charlson, R.J., S.E. Schwartz, J.M. Hales, R.D. Cess, J.A. Coakley, Jr., J.E. Hansen, and D.J. Hoffman, Climate forcing by anthropogenic aerosols, *Science, 255*, 423-430, 1992.

Chylek, P., and J.G.D. Wong, Erroneous use of the modified Kohler equation in clouds and aerosol physics applications, *J. Atmos. Sci., 55*, 1473-1477, 1998.

Corrigan, C.E., and T. Novakov, Cloud condensation nucleus activity of organic compounds: A laboratory study, *Atmos. Environ., 33*, 2661-2668, 1999.

DeMott, P.J., Y. Chen, S.M. Kreidenweis, D.C. Rogers, and D.E. Sherman, Ice formation by black carbon particles, *Geophys. Res. Lett , 26*, 2429-2432, 1999.

Dentener, F.J., G.R. Carmichael, Y. Zhang, J. Lelieveld, and P.J. Crutzen, Role of mineral aerosol as a reactive surface in the global troposphere, *J. Geophys Res., 101*, 22,869-22,889, 1996.

Facchini, M.C., et al., Partitioning of the organic aerosol component between fog droplets and interstitial air, *J Geophys. Res., 104*, 26,821-26,832, 1999.

Fitzgerald, J.W., and P.A. Spyers-Duran, Changes in cloud nucleus concentration and cloud droplet size distribution associated with pollution from St. Louis, *J. Appl. Meteorol., 12*, 511-516, 1973.

Ghan, S.J., G. Guzman, and H. Abdul-Razzak, Competition between sea-salt and sulfate particles as cloud condensation nuclei, *J. Atmos. Sci., 55*, 3340-3347, 1998.

Gras, J. L., CN, CCN and particle size in Southern Ocean air at Cape Grim, *Atmos. Res., 35*, 233-251, 1995.

Guazzotti, S.A., K.R. Coffee, and K.A. Prather, Realtime monitoring of size-resolved single particle chemistry during INDOEX-IFP 1999, in *European Aerosol Conference (Dublin) Abstract Volume*, vol. 31, pp. S182-S183, Pergamon, New York, 2000.

Han, Q., W. B. Rossow, and A.A. Lacis, Near-global survey of effective droplet radii in liquid water clouds using ISCCP data, *J. Clim., 7*, 465-497, 1994.

Heymsfield, A.J, and G.M. McFarquhar, Microphysics of INDOEX clean and polluted trade cumulus clouds, *J. Geophys. Res.*, this issue.

Hudson, J. G., Effects of CCN on stratus clouds, *J. Atmos. Sci., 40*, 480-486, 1983.

Hudson, J.G., An instantaneous CCN spectrometer, *J Atmos. Oceanic Technol*, *6*, 1055-1065, 1989.

Hudson, J.G., and S.S. Yum, Maritime/continental drizzle contrasts in small cumuli, *J. Atmos. Sci.*, in press, 2000a.

Laaksonen, A., P. Korhonen, M. Kulmala, and R.J. Charlson, Modification of the Kohler equation to include soluble trace gases and slightly soluble substances, *J. Atmos. Sci., 55*, 853-862, 1998.

Leaitch, W.R., G.A.Isaac., J.W. Strapp, C.M. Banic, and H.A. Wiebe, The relationship between cloud droplet number concentrations and anthropogenic pollution: Observations and climatic implications, *J Geophys. Res*, *97*, 2463-2472, 1992.

Martin, G.M., D.W. Johnson, and A. Spice, The measurement and parameterization of effective radius of droplets in warm stratocumulus clouds, *J. Atmos. Sci*, *51*, 1823-1842, 1994.

Massling, A., A. Weidensohler, B. Busch, T. Miller, D. Coffman, P. Quinn, T. Bates, and D. Covert, Soluble particle volume fractions derived from hygroscopic growth and chemical composition measurements during INDOEX, in *European Aerosol Conference (Dublin) Abstract Volume*, vol. 31, pp. S991-S994, Pergamon, New York, 2000.

McFarquhar, G.M., and A. J. Heymsfield, Parameterizations of INDOEX microphysical measurements and calculations of cloud susceptibility: Applications for climate studies, *J. Geophys. Res.*, this issue.

Nenes, A., P.Y. Chuang, R.C. Flagan, and J.H. Seinfeld, A theoretical analysis of cloud condensation nucleus (CCN) instruments, *J. Geophys Res.* in press, 2000.

Noone, K.J., J.A. Ogren, J. Heintzenberg, R.J. Charlson, and D.S. Covert, Design and calibration of a counterflow virtual impactor for sampling of atmospheric fog and cloud droplets, *Aerosol Sci. Technol., 8*, 235-244, 1988.

Novakov, T., and J.E. Penner, Large contribution of organic aerosols to cloud-condensation-nuclei concentrations, *Nature, 365*, 823-826, 1993.

O'Dowd, C.O., J.A. Lowe, and M.H. Smith, Coupling sea-salt and sulphate interactions and its impact on cloud droplet concentration predictions, *Geophys. Res. Lett., 26*, 1311-1314, 1999.

Ogren, J.A., and R.J. Charlson, Implications for models and measurements of chemical inhomogeneities among cloud droplets, *Tellus, Ser. B, 44*, 208-225, 1992.

Ogren, J.A., J. Heintzenberg, and R.J. Charlson, In-situ sampling with a droplet to aerosol converter, *Geophys. Res. Lett., 12*, 121-124, 1985.

Pinnick, R.G., J.D. Pendleton, and G. Videen, Response characteristics of the Particle Measuring Systems Active Scattering Aerosol Spectrometer Probes, *Aerosol Sci. Technol., 33*, 334-352, 2000.

Posfai, M., J.R. Anderson, P.R. Buseck, and H. Sievering, Compositional variations of sea-salt-mode aerosol particles from the North Atlantic, *J. Geophys. Res., 100*, 23,063-23,074, 1995.

Radke, L.F., J.A. Coakley, Jr. and M.D. King, Direct and remote sensing observations of the effects of ships on clouds, *Science, 246*, 1146-1148, 1989.

Sassen, K., D. Starr, G.C. Mace, M.R. Poellet, S.H. Melfi, W.L. Eberhard, J.D. Spinhirne, E.W. Eloranta, D.E. Hagen, and J. Hallett, The 5-6 December 1991 FIRE IFO jet stream cirrus case study: Possible influences of volcanic aerosols, *J. Atmos. Sci., 52*, 97-125, 1995.

Satheesh, S.K., K. Krishna Moorthy, and B.V. Krishna Murthy, Spatial gradients in aerosol characteristics over the Arabian Sea and Indian Ocean, *J. Geophys. Res., 103*, 26,183-26,192, 1998.

Squires, P., The growth of cloud drops by condensation, *Aust. J. Sci. Res*, *A5*, 59-86, 1952.

Twohy, C. H., and B. W. Gandrud, Electron microscope analysis of residual particles from aircraft contrails, *Geophys. Res. Lett., 25*, 1359-1362, 1998.

Twohy, C.H., and J.G. Hudson, Measurements of cloud condensation nucleus spectra within maritime cumulus cloud droplets: Implications for mixing processes, *J. Appl. Meteorol., 34*, 815-833, 1995.

Twohy, C.H., P.H. Austin, and R.J. Charlson, Chemical consequences of the initial diffusional growth of cloud droplets: A clean marine case, *Tellus, Ser B, 41*, 51-60, 1989.

Twohy, C.H, P.S. Durkee, B.J. Huebert, and R.J. Charlson, Effects of aerosol particles on the microphysics of coastal stratiform clouds, *J Clim*, *8*, 773-783, 1995.

Twohy, C.H., A.J. Schanot, and W.A. Cooper, Measurement of condensed water content in liquid and ice clouds using an airborne counterflow virtual impactor, *J. Atmos. Oceanic Technol., 14*, 197-202, 1997.

Twomey, S., The influence of pollution on the shortwave albedo of clouds, *J. Atmos. Sci., 34*, 1149-1152, 1977a.

Twomey, S., *Atmospheric Aerosols*, 302 pp., Elsevier Sci. , New York, 1977b.

Wetzel, M.A., and L.L. Stowe, Satellite-observed patterns in stratus microphysics, aerosol optical thickness, and shortwave radiative forcing, *J. Geophys. Res., 104*, 31,286-31,299, 1999.

Wexler, A.S., F.W. Lurmann, and J. H. Seinfeld, Modelling urban and regional aerosols, I, Model development, *Atmos. Environ., 28*, 531-546, 1994.

Yum, S. S., J.G. Hudson, and Y. Xie, Comparisons of cloud microphysics with cloud condensation nuclei spectra over the summertime Southern Ocean, *J Geophys. Res., 103*, 16,625-16,636, 1998.

J.R. Anderson, Department Mechanical and Aerospace Engineering, Arizona State University, Tempe, AZ 85287.

D. Baumgardner, Centro de Ciencias de las Atmosfera, UNAM, Ciudad Universitaria, Mexico City, 04510 Mexico DF.

S.K. Durlak, National Center for Atmospheric Research, Boulder, CO 80307.

J.G. Hudson and S.S. Yum, Atmospheric Sciences Division, Desert Research Institute, Reno, NV 89512.

C.H. Twohy, Department of Oceanic and Atmospheric Sciences, Oregon State University, Corvallis, OR 97331 (twohy@oce.orst.edu)

(Received July 6, 2000; accepted November 10, 2000.)